# Performance Comparison Between Continuous Aperture MIMO and Discrete MIMO

Zhongzhichao Wan, Jieao Zhu, and Linglong Dai, *Fellow, IEEE*
Department of Electronic Engineering, Tsinghua University
Beijing National Research Center for Information Science and Technology (BNRist), Beijing 100084, China
E-mails: {wzzc20, zja21}@mails.tsinghua.edu.cn; daill@tsinghua.edu.cn

***Abstract*—The concept of continuous-aperture multiple-input multiple-output (CAP-MIMO) technology has been proposed recently, which aims at achieving high spectrum efficiency by deploying extremely dense antennas or even continuous antennas in a given aperture. The fundamental question of CAP-MIMO is whether it can achieve much better performance than the traditional discrete MIMO system. In this paper, we propose a non-asymptotic performance comparison scheme between continuous and discrete MIMO systems based on the analysis of mutual information. We show the consistency of the proposed scheme by proving that the mutual information between discretized transceivers converges to that between continuous transceivers. Numerical analysis verifies the theoretical results, and suggests that the mutual information obtained from the discrete MIMO with widely adopted half-wavelength spaced antennas almost achieves the mutual information obtained from CAP-MIMO.**

***Index Terms*—Multiple-input multiple-output (MIMO), Continuous-aperture MIMO (CAP-MIMO), mutual information, random fields, Fredholm determinant.**

## I. Introduction

The spectrum efficiency of wireless communication systems has been greatly improved from 3G to 5G because of the use of multiple-input multiple-output (MIMO) technology [1]–[3]. Along with the tendency of increasing the number of antennas to achieve higher spectrum efficiency, people are considering deploying extremely dense antennas or even continuous antenna in a given aperture [4], [5]. The MIMO with extremely dense antennas is called continuous-aperture MIMO (CAP-MIMO), and is also called holographic MIMO [6]–[8] or large intelligent surface [4], [9] in the recent literature. It has attracted increasing interest in the research of MIMO technology. Recent works about CAP-MIMO include pattern optimization [5], antenna design [10], channel estimation [6], and so on. For CAP-MIMO, the fundamental question is whether the CAP-MIMO system can achieve much better performance than the traditional discrete MIMO system.

### A. Related works

There are many structures with different antenna spacing for realizing the discrete MIMO. Therefore, we need to choose which structure of the discrete MIMO to compare with CAP-MIMO. A representative structure of discrete MIMO uses half-wavelength spaced antennas to compose the transceivers [11]–[13], because half-wavelength sampling of the electromagnetic field can reconstruct the original field according to the sampling theorem.

979-8-3503-1090-0/23/$31.00 © 2023 IEEE

There have been several works discussing the performance comparison between CAP-MIMO and discrete MIMO with half-wavelength spaced antennas from the perspective of degree of freedom (DoF). According to the Nyquist sampling theorem [14], half-wavelength sampling for a field observed in the infinitely large region can perfectly recover the original field [15]. For a rigorous analysis framework of the DoF in a *finitely* large aperture, the prolate spheroidal wave function (PSWF) [16] is introduced to perform orthogonal expansion on the electromagnetic field. Such an electromagnetic field observed in a *finitely* large region can be approximately reconstructed from a finite number of PSWFs. If the reconstruction error can be controlled within a given threshold by using $N_0$ PSWFs, the number of DoFs of the field can be approximated by $N_0$ [17].

This analyzing scheme is strict, but can only provide the **asymptotic** result of the DoF, i.e., the quantitative result of $N_0$ can be obtained only when the length of the region or the frequency tends to infinity. Under this assumption, $N_0$ equals the number of antennas under half-wavelength sampling. However, the practical systems are with finitely large aperture and finite frequency. The **asymptotic** result can not provide quantitative number of DoFs for practical systems. Therefore, a **non-asymptotic** performance comparison scheme between CAP-MIMO and discrete MIMO is required for the accurate performance comparison with finitely large apertures.

### B. Our contributions

To solve this problem, in this paper, we provide a **non-asymptotic** performance comparison scheme between CAP-MIMO and discrete MIMO, and we further prove the rationality of the scheme. Specifically, the contributions of this paper can be summarized as follows:

- We build models of CAP-MIMO and discrete MIMO based on electromagnetic theory. For CAP-MIMO with continuous transceivers, we model the structural characteristics of the continuous random electromagnetic fields from physical laws by using self-adjoint operators. Based

on this model, we can utilize the spectrum theory of operators to derive the information that can be obtained from the received field. The existing models of MIMO with discrete transceivers are spatially discretized from the continuous model. Moreover, signal-to-noise ratio (SNR) control schemes are introduced to ensure the fairness of the comparison between CAP-MIMO and discrete MIMO.

- Then, we prove that the mutual information between the discrete transceivers converges to the mutual information between continuous transceivers when the number of antennas of the discretized transceivers tends to infinity. Therefore, the continuous model in our paper is compatible with the existing discrete models, and the fairness of the performance comparison is guaranteed. Numerical results are provided to verify the theoretical analysis. Moreover, it shows the near-optimality of the half-wavelength sampling of the transceivers in traditional discrete MIMO.

*Notation*: bold characters denote matrices and vectors; j is the imaginary unit; $\mathbb{E}[x]$ denotes the mean of random variable $x$; $x^*$ denotes the conjugation of a number or a function $x$; $\mathbf{X}^{\mathrm{H}}$ denotes the conjugate transpose of a vector or a matrix $\mathbf{X}$; $|\phi\rangle$ is the quantum mechanical notation of a function $\phi$, where the inner product is denoted by $\langle\psi|\,\phi\rangle$; $\det(\cdot)$ denotes the matrix determinant or the Fredholm determinant; $\mathrm{tr}(\cdot)$ denotes the trace of a matrix or an operator. $\mathbf{I}_m$ denotes the $m\times m$ identity matrix, $\mathbf{1}$ denotes the identity operator, $\delta(x)$ denotes the delta function, and $\mathbb{1}_{i=j}$ denotes the indicator function; $|x|$ denotes the modulus of a complex variable, and $\|f(x)\|_{L^\infty(a,b)}$ is the uniform norm of the function $f(x)$ over the interval $[a,b]$. $C^\infty(K)$ denotes the set of smooth functions supported on a compact set $K$.

## II. Models of continuous and discrete systems

In this section, we introduce the models of continuous and discrete systems for performance comparison between CAP-MIMO and discrete MIMO. We control the SNR at the receiver side to ensure the fairness of the comparison. The information obtained from these models is derived from operators and matrices.

### A. Basic model of electromagnetic information theory

To model the transceivers and the channel, we follow the approach of electromagnetic information theory (EIT). The EIT is an interdisciplinary subject that integrates the classical electromagnetic theory and information theory to build an analysis framework for the ultimate performance bound of wireless communication systems [18]. The analysis framework of EIT is based on spatially continuous electromagnetic fields, which provides us the tool to model and analyze the continuous transceivers. Then, for the consistency, the model of discrete transceivers are viewed as the discretization of the continuous model from EIT.

The model of EIT is built on the vector wave equation [19] without boundary conditions, which is expressed by

$$\nabla\times\nabla\times\mathbf{E}(\mathbf{r})-\kappa_0^2\mathbf{E}(\mathbf{r})=\mathrm{j}\omega\mu_0\mathbf{J}(\mathbf{r})=\mathrm{j}\kappa_0 Z_0\mathbf{J}(\mathbf{r}), \quad (1)$$

where $\kappa_0=\omega\sqrt{\mu_0\varepsilon_0}$ is the wavenumber, and $Z_0=\mu_0 c=120\pi\,[\Omega]$ is the free-space intrinsic impedance.

We assume that the transceivers are confined in two regions $V_{\mathrm{s}}$ and $V_{\mathrm{r}}$, separately. The current density at the source is $\mathbf{J}(\mathbf{s})$, where $\mathbf{s}\in\mathbb{R}^3$ is the coordinate of the source. The induced electric field at the destination is $\mathbf{E}(\mathbf{r})$, where $\mathbf{r}\in\mathbb{R}^3$ is the coordinate of the field observer. To solve the vector wave equation, a general theoretical approach is to introduce the dyadic Green's function $\mathbf{G}(\mathbf{r},\mathbf{s})\in\mathbb{C}^{3\times3}$. The electric field $\mathbf{E}(\mathbf{r})$ can be expressed by $\mathbf{E}(\mathbf{r})=\int_{V_s}\mathbf{G}(\mathbf{r},\mathbf{s})\mathbf{J}(\mathbf{s})\mathrm{d}\mathbf{s},\quad \mathbf{r}\in V_r$. By exploiting the symmetric properties of the free space, the Green's function in unbounded, homogeneous mediums at a fixed frequency point is [20]

$$\mathbf{G}(\mathbf{r},\mathbf{s})=\frac{\mathrm{j}\kappa_0 Z_0}{4\pi}\left(\mathbf{I}+\frac{\nabla_{\mathbf{r}}\nabla_{\mathbf{r}}^{\mathrm{H}}}{\kappa_0^2}\right)\frac{e^{\mathrm{j}\kappa_0\|\mathbf{r}-\mathbf{s}\|}}{\|\mathbf{r}-\mathbf{s}\|}, \quad (2)$$

where $\hat{\mathbf{p}}=\frac{\mathbf{p}}{\|\mathbf{p}\|}$ and $\mathbf{p}=\mathbf{r}-\mathbf{s}$.

Since there are some non-ideal factors at the receiver that corrupts the received field, we call them the noise field $\mathbf{N}(\mathbf{r})$. The received electric field can be expressed by $\mathbf{Y}(\mathbf{r})=\mathbf{E}(\mathbf{r})+\mathbf{N}(\mathbf{r})$. The above equations represent the deterministic model in the electromagnetic theory. To satisfy the demand of wireless communication, we need to convey information through the electromagnetic field. Specifically, the wireless communication system encodes the information in the current $\mathbf{J}(\mathbf{s})$, and decodes the information from the noisy electric field $\mathbf{Y}(\mathbf{r})$. Due to the randomness of the transmitted bit source, the electromagnetic fields are randomly excited by the transmitter equipment before being radiated into the propagation media. Therefore, the electromagnetic fields should be modeled as random fields [21], and we adopt the Gaussian random fields to depict the statistical characteristics of the fields. We denote the autocorrelation function of the current and the electric field as matrix-valued functions $\mathbf{R}_{\mathbf{J}}(\mathbf{s},\mathbf{s}')=\mathbb{E}[\mathbf{J}(\mathbf{s})\mathbf{J}^{\mathrm{H}}(\mathbf{s}')]$ and $\mathbf{R}_{\mathbf{E}}(\mathbf{r},\mathbf{r}')=\mathbb{E}[\mathbf{E}(\mathbf{r})\mathbf{E}^{\mathrm{H}}(\mathbf{r}')]$. The relationship between $\mathbf{R}_{\mathbf{J}}$ and $\mathbf{R}_{\mathbf{E}}$ is determined by the Green's function, which is

$$\mathbf{R}_{\mathbf{E}}(\mathbf{r},\mathbf{r}')=\int_{V_s}\int_{V_s}\mathbf{G}(\mathbf{r},\mathbf{s})\mathbf{R}_{\mathbf{J}}(\mathbf{s},\mathbf{s}')\mathbf{G}^{\mathrm{H}}(\mathbf{r},\mathbf{s})\mathrm{d}\mathbf{s}\mathrm{d}\mathbf{s}'. \quad (3)$$

Similar definitions of the autocorrelation functions for the noise field and the noisy electric field are represented as $\mathbf{R}_{\mathbf{N}}(\mathbf{r},\mathbf{r}')=\mathbb{E}[\mathbf{N}(\mathbf{r})\mathbf{N}^{\mathrm{H}}(\mathbf{r}')]$ and $\mathbf{R}_{\mathbf{Y}}(\mathbf{r},\mathbf{r}')=\mathbb{E}[\mathbf{Y}(\mathbf{r})\mathbf{Y}^{\mathrm{H}}(\mathbf{r}')]$.

### B. Continuous transceivers

In this part, we will build the model of CAP-MIMO with continuous transceivers based on the EIT model in the above subsection, and then derive the mutual information between the continuous transceivers. For simplicity, in the rest part of the

paper, we assume that the transceivers are linear along the $\hat{z}$-direction. Moreover, since the current $J$ can only exist on the linear source and we only observe the electric field on the linear receiver, we express all the physical quantities in a Cartesian coordinate system that satisfies $\mathbf{s} = (0, 0, s)$ and $\mathbf{r} = (d, 0, r)$, where $d$ is the distance between the parallel source and destination line. This model corresponds to single-polarized linear antennas. Through this simplification scheme, we use $J(s)$ and $E(r)$ instead of $\mathbf{J}(\mathbf{s})$ and $\mathbf{E}(\mathbf{r})$. The relationship between them can be expressed by $E(r) = \int_0^l G(r, s)J(s)\mathrm{d}s$, where $G(r, s)$ is the bottom-right element of the matrix $\mathbf{G}(\mathbf{r}, \mathbf{s})$, i.e., $G = \mathbf{G}_{3,3}$. We can derive $G(r, s)$ as

$$\begin{aligned} G(r,s) =& \frac{\mathrm{j}Z_0 e^{\mathrm{j}2\pi\sqrt{x^2+d^2}/\lambda}}{2\lambda\sqrt{x^2+d^2}}\Big[\frac{\mathrm{j}}{2\pi\sqrt{x^2+d^2}/\lambda}\frac{d^2-2x^2}{x^2+d^2} \\ &+ \frac{d^2}{x^2+d^2} - \frac{1}{(2\pi/\lambda)^2(x^2+d^2)}\frac{d^2-2x^2}{x^2+d^2}\Big], \end{aligned} \tag{4}$$

where $x = r - s$ and $\lambda = 2\pi/\kappa_0$ is the wavelength.

Here we consider the scenario with no channel state information, which means that the signals on the source are under equal power allocation. The second moments (autocorrelation) of $J$ are denoted by $R_J(s, s') = P\delta(s - s'), s, s' \in [0, l]$. Since the noiseless received field is uniquely determined by the source and the deterministic channel, the autocorrelation function of the electric field is expressed by the source autocorrelation $R_J(s, s')$ and the Green's function $G(r, s)$, written as $R_E(r, r') = P\int_0^l G(r, s)G^*(r', s)\mathrm{d}s$.

The received field on the destination is $Y(r) = E(r)+N(r)$, where $N(r)$ is the noise field at the receiver. In this paper, we consider thermal noise model $\mathbb{E}\left[N(r)N^*(r')\right] = \frac{n_0}{2}\delta(r - r')$. According to [22], we can perform Mercer expansion on the electric field $E(r)$ to obtain a set of mutually independent random variables $\xi_k$. The expansion can be written as $E(r) = \sum_k \xi_k\phi_k(r)$, where $\mathbb{E}[\xi_{k_i}\xi^*_{k_j}] = \lambda_{k_i}\mathbb{1}_{i=j}$ and $\langle\phi_{k_i}(r)|\phi_{k_j}(r)\rangle = \delta_{k_ik_j}$. This expansion scheme has split the continuous field into independent components. Since the white noise field can be expanded under arbitrary orthogonal bases, the continuous channel is also decomposed into independent subchannels, which makes the mutual information of the subchannels summable.

For the self-adjoint operator $T_E := \phi(r) \to \int_0^l K_E(r, r')\phi(r')\mathrm{d}r'$, where $K_E(r, r') = R_E(r, r') = P\int_0^l G(r, s)G^*(r', s)\mathrm{d}s$, all of its eigenvalues are real and nonnegative. From [23] we know that an integral operator on $[a, b]$ is a trace class operator if its kernel $K(x, y)$ satisfies $K(x, y)$ and $\partial_y K(x, y)$ are continuous on $[a, b]^2$. Therefore $T_E$ is a trace class operator, which means that the sum of its eigenvalues is finite and can be expressed by [24]

$$\mathrm{tr}(T_E) = \int_0^l K_E(r, r)\mathrm{d}r = P\int_0^l\int_0^l G(r, s)G^*(r, s)\mathrm{d}r\mathrm{d}s. \tag{5}$$

**Corollary 1:** The non-negative values $\frac{\lambda_k}{n_0/2}$ represent the SNR of the independent subchannels. The mutual information between the noisy received field and the current on the source can be expressed by

$$I_0(J;Y) = \sum_{k=1}^{+\infty}\log\left(1 + \frac{\lambda_k}{n_0/2}\right). \tag{6}$$

By introducing the Fredholm determinant which is the determinant of operators [25], we can express (6) by $I_0(J;Y) = \log\det\left(\mathbf{1} + \frac{T_E}{n_0/2}\right)$, where $(T_E\phi)(r) := \int_0^L R_E(r, r')\phi(r')\mathrm{d}r'$ and $\lambda_k$ are the eigenvalues of $T_E$.

### C. Discrete transceivers

In this subsection, we will introduce a model which discretizes the transceivers simultaneously. Specifically, we build a model with $m_1$ point antennas on a length-$l$ segment in the source region and $m_2$ point antennas on a length-$l$ segment in the destination region. We assume that the $i_{\mathrm{th}}$ point antenna is placed at $s_i$ in the source region and $r_i$ in the destination region. The correlation matrix of the signals in the source region is set to be an identity matrix $\mathbf{K}'_J = P\mathbf{I}_{m_1}$, which corresponds to the power allocation scheme with no channel state information at the transmitter. The channel gain from the $i_{\mathrm{th}}$ antenna in the source region and the $j_{\mathrm{th}}$ antenna in the destination region can be expressed by $\mathbf{H}_{i,j} = G(r_i, s_j)$. The correlation matrix of the received signal is denoted by $\mathbf{K}'_E = \mathbf{H}\mathbf{K}'_J\mathbf{H}^{\mathrm{H}}$. The noise matrix is denoted by $\mathbf{K}'_N = \frac{n_1}{2}\mathbf{I}_{m_2}$.

We control the signal-to-noise ratio (SNR) of this model the same as that of the continuous model to ensure the fairness of the comparison. The SNR at the receiver of the continuous model is $\sum_{i=1}^{\infty}\frac{\lambda_i}{n_0/2}$, where $\lambda_i$ is the $i_{\mathrm{th}}$ eigenvalue of the operator $T_E$. From (5) we know that $\sum_{i=1}^{\infty}\frac{\lambda_i}{n_0/2} = \frac{P}{n_0/2}\int_0^l\int_0^l G(r, s)G^*(r, s)\mathrm{d}r\mathrm{d}s$ is finite. The SNR at the receiver of the discrete model is $\sum_{i=1}^{m_2}\frac{\lambda'_i}{n_1/2}$, where $\lambda'_i$ is the $i_{\mathrm{th}}$ eigenvalue of the matrix $\mathbf{K}'_E$. Then, we have $\sum_{i=1}^{\infty}\frac{\lambda_i}{n_0/2} = \sum_{i=1}^{m_2}\frac{\lambda'_i}{n_1/2}$, which leads to

$$n_1 = n_0\frac{\sum_{i=1}^{m_2}\sum_{j=1}^{m_1}G(r_i, s_j)G^*(r_i, s_j)}{\int_0^l\int_0^l G(r, s)G^*(r, s)\mathrm{d}r\mathrm{d}s}. \tag{7}$$

We denote the determinant of matrix $\mathbf{K} \in \mathbb{C}^{m\times m}$ by $\det(\mathbf{K}_{i,j})_{i,j=1}^m$. The mutual information between the transceivers is expressed as:

$$\begin{aligned} I_1 &= \log\left(\frac{\det(\mathbf{K}'_N + \mathbf{K}'_E)}{\det(\mathbf{K}'_N)}\right) \\ &= \mathrm{logdet}\left(\mathbb{1}_{i=j} + \frac{\sum_{k=1}^{m_1}G(r_i, s_k)G^*(r_j, s_k)}{n_1/2}\right)_{i,j=1}^{m_2}. \end{aligned} \tag{8}$$

## III. Comparison between continuous and discrete transceivers

In the above section we have built the models with continuous and discrete transceivers. In this section we will compare the mutual information between continuous transceivers and that between discrete transceivers. Numerical analysis is then provided to verify the theoretical analysis, and show the near-optimality of the half-wavelength sampling scheme.

### A. Convergence analysis of the mutual information

The analysis in this section focuses on the difference between $I_0$ and $I_1$. We define $I_0^{'} = \text{logdet}\left(\mathbf{1} + \frac{m_1 m_2 T_E}{l^2 n_1/2}\right)$ as an intermediate variable.

First we will use the following lemma to show the error bound of a multivariate quadrature rule, which is a direct deduction from [26]

**Lemma 1:**

$$\begin{aligned}&\left|Q_m^n(K_n) - \int_{[0,l]^n} K_n(x_1,\cdots,x_n)\mathrm{d}x_1\cdots\mathrm{d}x_n\right| \\ &\leqslant l^{n-1}\sum_{i=1}^{n} E_i,\end{aligned} \tag{9}$$

where $Q_m^n(K_n) = \sum_{j_1,\cdots,j_n=1}^{m}\prod_{i=1}^{n} w_{j_i} K_n(r_{j_1},\cdots,r_{j_n})$ is the multivariate numerical approximation of the integral, $E_i = \left|Q_i(K_n;x_i) - \int_0^l K_n(x_1,\cdots,x_n)\mathrm{d}x_i\right|$ is the approximation error of the integral on one variable, and $Q_i(K_n;x_i) := \sum_{j_i} w_{j_i} K_n(x_1,\cdots,x_i = r_{j_i},\cdots,x_n)$.

Then we will use **Lemma 1** to discuss the convergence of $|I_0 - I_0^{'}|$ in the following lemma:

**Lemma 2:** The mutual information $I_0^{'}$ converges to the mutual information $I_0$. The difference $\left|I_0 - I_0^{'}\right|$ is at most inverse-proportional to $(\min(m_1,m_2))^2$.

*Proof:* From the SNR control scheme of discrete transceivers (7) and the multivariate $m$-point composite midpoint quadrature rule, we have (10) where $g(x,y,z) := G(x,z)G^*(y,z)$, $r_i = (i-0.5)l/m_2$, and $s_j = (j-0.5)l/m_1$. It is obvious that $n_1/(m_1m_2)$ converges to $n_0/l^2$ when $m_1 \to \infty$ and $m_2 \to \infty$. We denote the minimum value of $n_1/(m_1m_2)$ by $c$.

Since the Fredholm determinant $f(z) = \det(\mathbf{1} + zT_E)$ is an analytic function, we know from mean value theorem that $\exists x \in [\min(z,z_1),\max(z,z_1)]$:

$$\begin{aligned}&|\det(\mathbf{1} + zT_E) - \det(\mathbf{1} + z_1T_E)| \\ &= |z - z_1|\left|\frac{\partial\det(\mathbf{1} + xT_E)}{\partial x}\right|.\end{aligned} \tag{11}$$

In our assumption $z = \frac{2}{n_0}$ and $z_1 = \frac{2m_1m_2}{l^2n_1}$. We have that

$$|z - z_1| \leqslant \frac{2}{n_0 l^2 c}|n_0 - \frac{l^2}{m_2m_1}n_1|. \tag{12}$$

The analycity of $\det(\mathbf{1} + zT_E)$ implies that $\frac{\partial\det(\mathbf{1}+xT_E)}{\partial x}$ is also an analytic function and is bounded on the interval $[\min(z,z_1),\max(z,z_1)]$.

Then, according to (11), we know that $\left|\det(\mathbf{1} + \frac{2}{n_0}T_E) - \det(\mathbf{1} + \frac{2m_1m_2}{l^2n_1}T_E)\right|$ converges to 0 when $m_1 \to \infty$ and $m_2 \to \infty$. For $|I_0 - I_0^{'}|$ we have

$$|I_0 - I_0^{'}| \leqslant \frac{|\det(\mathbf{1} + \frac{2}{n_0}T_E) - \det(\mathbf{1} + \frac{2m_1m_2}{l^2n_1}T_E)|}{\min(\det(\mathbf{1} + \frac{2}{n_0}T_E),\det(\mathbf{1} + \frac{2m_1m_2}{l^2n_1}T_E))}. \tag{13}$$

Therefore, $|I_0 - I_0^{'}|$ converges to 0, and the difference is at most inversely proportional to $(\min(m_1,m_2))^2$. ∎

After clarifying that $I_0^{'}$ converges to $I_0$, we introduce the following lemma from [27]:

**Lemma 3:** Define $d(z) := \det(\mathbf{1} + zT)$ and $d_Q(z) := \det\left(\mathbb{1}_{i=j} + w_j z K(r_i,r_j)\right)_{i,j=1}^{m}$, where $K$ is the kernel of the integral operator $T := \phi(x) \to \int_{[a,b]} K(x,y)\phi(y)\mathrm{d}y$. The difference between $d(z)$ and $d_Q(z)$ is

$$\begin{aligned}d(z) - d_Q(z) = \sum_{n=1}^{\infty}\frac{z^n}{n!}\Bigg(&Q_m^n(K_n) \\ &- \int_{[a,b]^n} K_n(x_1,\cdots,x_n)\mathrm{d}x_1\cdots\mathrm{d}x_n\Bigg),\end{aligned} \tag{14}$$

where $K_n(x_1,\cdots,x_n) = \det\left(K(x_i,x_j)\right)_{i,j=1}^{n}$, and $Q_m^n(K_n) = \sum_{j_1=1,\cdots,j_n=1}^{m}\prod_{i=1}^{n} w_{j_i} K_n(r_{j_1},\cdots,r_{j_n})$.

Then we will discuss the convergence of $|I_1 - I_0^{'}|$ in the following lemma:

**Lemma 4:** The difference $\left|I_1 - I_0^{'}\right|$ approaches 0 when $m$ approaches infinity. Moreover, it is at most inverse-proportional to $(\min(m_1,m_2))^2$.

*Proof:* The main idea of the proof is to introduce the Fredholm determinant and its discretization by $d(z) = \det(\mathbf{1} + zT)$ and $d_V(z) = \det\left(\mathbb{1}_{i=j} + w_j' z\sum_{k=1}^{m_1} w_k G(r_i,s_k)G^*(r_j,s_k)\right)_{i,j=1}^{m_2}$, where $K(x_i,x_j) = \int_0^l G(x_i,s)G^*(x_j,s)\mathrm{d}s$ is the kernel of the operator $T$. Note that $d_V(z)$ is a further discretization on $d_Q(z)$ in **Lemma 3** by discretizing $K(r_i,r_j)$. Through some mathematical tricks, we can bound the difference between $d(z)$ and $d_V(z)$ by using **Lemma 1**, **Lemma 3** and other tools like the Hadamard's inequality [28]. For space limitation, the detailed proof is omitted. ∎

Therefore, we have **Theorem 1**:

**Theorem 1:** The mutual information $I_1$ that can be obtained from the discrete transceivers converges to the mutual information $I_0$ that can be obtained from the continuous transceivers when the number of antennas in the discrete transceivers increases. The difference $|I_0 - I_1|$ is at most inverse-proportional to the square of $m$, where $m = \min(m_1,m_2)$.

**Remark 1:** Insight about the sampling numbers: **Theorem 1** reveals the convergence of $|I_0 - I_1|$ with respect to $m = \min(m_1,m_2)$. It shows that the mutual information of

$$\begin{aligned}
&\left|n_0 - \frac{l^2}{m_2 m_1} n_1\right| = \frac{n_0}{\int_0^l K(r,r)\mathrm{d}r} \left| \int_0^l \int_0^l g(r,r,s)\mathrm{d}s\mathrm{d}r - \frac{l^2}{m_1 m_2} \sum_{i=1,j=1}^{m_2,m_1} g(r_i, r_i, s_j) \right| \\
&\leqslant \frac{n_0 l^4}{24 m_2^2 \int_0^l K(r,r)\mathrm{d}r} \left\| \frac{\partial^2 g(r,r,s)}{\partial r^2} \right\|_{L^\infty((0,l)^2)} + \frac{n_0 l^4}{24 m_1^2 \int_0^l K(r,r)\mathrm{d}r} \left\| \frac{\partial^2 g(r,r,s)}{\partial s^2} \right\|_{L^\infty((0,l)^2)} \\
&\leqslant \frac{n_0 l^4}{24 (\min(m_1,m_2))^2 \int_0^l K(r,r)\mathrm{d}r} \left( \left\| \frac{\partial^2 g(r,r,s)}{\partial r^2} \right\|_{L^\infty((0,l)^2)} + \left\| \frac{\partial^2 g(r,r,s)}{\partial s^2} \right\|_{L^\infty((0,l)^2)} \right),
\end{aligned} \tag{10}$$

the discrete MIMO system depends on both sampling numbers $m_1$ and $m_2$ of the transceivers. They have some symmetry in (10), which we will show further in the numerical analysis. Moreover, if $m_2 > m_1$, then increasing $m_2$ while $m_1$ is fixed will not apparently increase the mutual information that can be obtained. Therefore, for mutual information, there is a short board effect in the discretization of transceiver with dense antennas.

**Remark 2:** Extension to other scenarios with power allocation: The convergence analysis in this section is not limited to the scenario with equal power allocation. For arbitrary analytic function $R_J(s,s')$, the convergence of $|I_0 - I_1|$ can be obtained. Instead of discretizing $\int G(r,z)G^*(r',z)\mathrm{d}z$ to $\sum_i G(r,r_i)G^*(r',r_i)$, we will discretize $\iint G(r,z)R_J(z,z')G^*(r',z')\mathrm{d}z\mathrm{d}z'$ to $\sum_{i,j} G(r,r_i)R_J(r_i,r_j)G^*(r',r_j)$ in the extended scenarios with power allocation schemes. Then, instead of $g(x,y,z)$ we need a four-variable function $h(x,y,z,\omega) := G(x,z)R_J(z,\omega)G^*(y,\omega)$ and the derivation procedure of the convergence has no essential difference with **Theorem 1** if the smoothness of $h(x,y,z,\omega)$ is guaranteed.

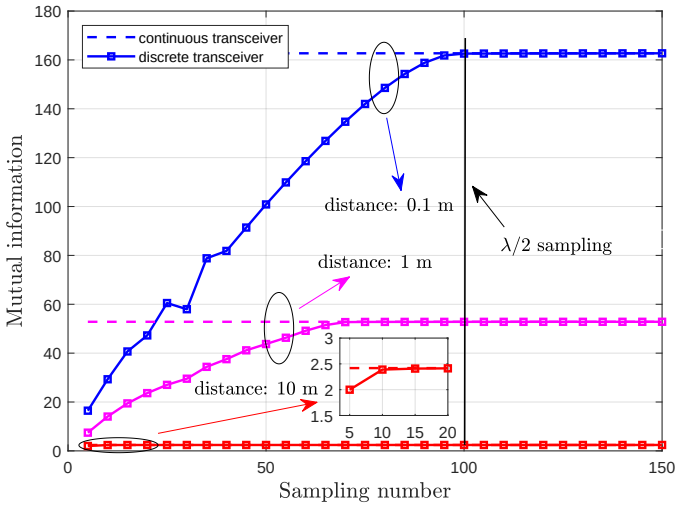


Fig. 1. The mutual information as a function of the sampling numbers, where the transceivers are with same sampling numbers.

### *B. Numerical analysis about the mutual information*

In this subsection, we will verify the correctness of the convergence analysis in the above subsection by simulations. The length $l$ of the transceivers is fixed to 2 m. The wavelength of the electromagnetic field is fixed to 0.04 m, which corresponds to the frequency of 7.5 GHz.

First we will discuss the scenario where the transceivers are both discretized to $m$ point antennas. The simulation results are shown in Fig. 1. From the simulation, we can observe the convergence of the mutual information between the discrete transceivers, which verifies the theoretical analysis. For the three distances between transceivers, the half-wavelength sampling almost achieves the supremum mutual information between continuous transceivers.

Then, in Fig. 2, we show the change of mutual information with respect to both $m_1$ and $m_2$, which are the sampling number of the transceivers. The distance $d$ is 1 m. We can find that, as we have predicted in **Remark 1**, the figure is approximately symmetric for $m_1$ and $m_2$. When we change the sampling

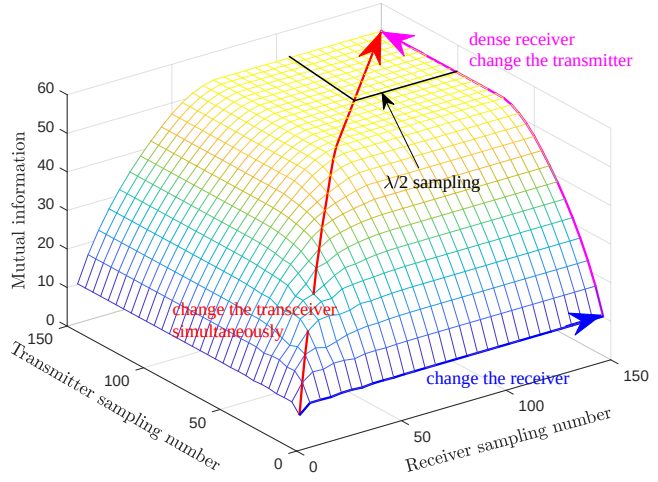


Fig. 2. The mutual information as a function of the sampling numbers of the transmitter and the receiver.

numbers of the transceivers simultaneously, the mutual information increases obviously as the red line shows. When the $m_2$ is large enough in the rosy line, which corresponds to dense antennas in the receiver, the mutual information will also increase with $m_1$. When $m_1$ or $m_2$ is small, which corresponds to sparse antennas, increasing the other sampling number only has a slight improvement on the mutual information, as the blue line shows. Therefore, the shortboard effect determines how the sampling numbers influence the mutual information. Moreover, the near-optimality of the half-wavelength sampling transceivers is also shown in Fig. 2.

## IV. Conclusion

In this paper, we proposed a comparison scheme between continuous and discrete MIMO systems which is based on a precise non-asymptotic analysis framework. We proposed physically consistent SNR control schemes to ensure the fairness of the comparison, and proved that the mutual information between discrete MIMO transceivers converges to that between continuous electromagnetic transceivers. Numerical results verified the theoretical analysis and showed the near-optimality of the half-wavelength sampling scheme.

Further works can be done by considering the mutual coupling of the antennas. The analysis based on the capacity after water-filling of the mutual information also remains to be explored.

## Acknowledgment

This work was supported in part by the National Key Research and Development Program of China (Grant No. 2020YFB1807201), in part by National Natural Science Foundation of China (Grant No. 62031019), and in part by the European Commission through the H2020-MSCA-ITN META WIRELESS Research Project under Grant 956256.

## References

[1] J. G. Andrews, S. Buzzi, W. Choi, S. V. Hanly, A. Lozano, A. C. K. Soong, and J. C. Zhang, "What will 5G be?" *IEEE J. Sel. Areas Commun.*, vol. 32, no. 6, pp. 1065–1082, Jun. 2014.

[2] F. Boccardi, R. W. Heath, A. Lozano, T. L. Marzetta, and P. Popovski, "Five disruptive technology directions for 5G," *IEEE Commun. Mag.*, vol. 52, no. 2, pp. 74–80, Feb. 2014.

[3] J. G. Andrews, X. Zhang, G. D. Durgin, and A. K. Gupta, "Are we approaching the fundamental limits of wireless network densification?" *IEEE Commun. Mag.*, vol. 54, no. 10, pp. 1558–1896, Oct. 2016.

[4] N. Decarli and D. Dardari, "Communication modes with large intelligent surfaces in the near field," *IEEE Access*, vol. 9, pp. 165 648–165 666, Dec. 2021.

[5] Z. Zhang and L. Dai, "Pattern-division multiplexing for continuous-aperture mimo," in *Proc. 2022 IEEE International Conference on Communications (ICC'22)*, May 2022, pp. 3287–3292.

[6] Ö. Demir, E. Björnson, and L. Sanguinetti, "Channel modeling and channel estimation for holographic massive MIMO with planar arrays," *IEEE Wireless Commun. Lett.*, Feb. 2022.

[7] A. Pizzo, T. L. Marzetta, and L. Sanguinetti, "Spatially-stationary model for holographic MIMO small-scale fading," *IEEE J. Sel. Areas Commun.*, vol. 38, no. 9, pp. 1964–1979, Sep. 2020.

[8] L. Sanguinetti, A. A. D'Amico, and M. Debbah, "Wavenumber-division multiplexing in line-of-sight holographic MIMO communications," *IEEE Trans. Wireless Commun.*, early access, Sep. 2022, doi: 10.1109/TWC.2022.3208961.

[9] J. Yuan, H. Q. Ngo, and M. Matthaiou, "Towards large intelligent surface (LIS)-based communications," *IEEE Trans. Commun.*, vol. 68, no. 10, pp. 6568–6582, Oct. 2020.

[10] O. Yurduseven, D. L. Marks, T. Fromenteze, and D. R. Smith, "Dynamically reconfigurable holographic metasurface aperture for a mills-cross monochromatic microwave camera," *Opt. Express*, vol. 26, no. 5, p. 5281–5291, Feb. 2018.

[11] Y. Sun, Z. Gao, H. Wang, B. Shim, G. Gui, G. Mao, and F. Adachi, "Principal component analysis-based broadband hybrid precoding for millimeter-wave massive MIMO systems," *IEEE Trans. Wireless Commun.*, vol. 19, no. 10, pp. 6331–6346, Oct. 2020.

[12] H. Zhang, N. Shlezinger, F. Guidi, D. Dardari, M. F. Imani, and Y. C. Eldar, "Beam focusing for near-field multi-user MIMO communications," *IEEE Trans. Wireless Commun.*, vol. 21, no. 9, pp. 7476–7490, Sep. 2022.

[13] Q. Wu and R. Zhang, "Intelligent reflecting surface enhanced wireless network via joint active and passive beamforming," *IEEE Trans. Wireless Commun.*, vol. 18, no. 11, pp. 5394–5409, Aug. 2019.

[14] H. Landau, "Sampling, data transmission, and the Nyquist rate," *Proc. IEEE*, vol. 55, no. 10, pp. 1701–1706, Oct. 1967.

[15] M. D. Migliore, "Near field antenna measurement sampling strategies: From linear to nonlinear interpolation," *Electronics*, vol. 7, no. 10, p. 257, Sep. 2018.

[16] D. Slepian and H. O. Pollak, "Prolate spheroidal wave functions, Fourier analysis and uncertainty—I," *Bell System Techn. Journal*, vol. 40, no. 1, pp. 43–63, Jan. 1961.

[17] F. Massimo, *Wave Theory of Information*. Cambridge, U.K.: Cambridge Univ. Press, 2017.

[18] J. Zhu, Z. Wan, L. Dai, M. Debbah, and H. V. Poor, "Electromagnetic information theory: Fundamentals, modeling, applications, and open problems," arXiv preprint arXiv:2212.02882, Dec. 2022.

[19] D. Dardari, "Communicating with large intelligent surfaces: Fundamental limits and models," *IEEE J. Sel. Areas Commun.*, vol. 38, no. 11, pp. 2526–2537, Nov. 2020.

[20] A. S. Poon, R. W. Brodersen, and D. N. Tse, "Degrees of freedom in multiple-antenna channels: A signal space approach," *IEEE Trans. Inf. Theory*, vol. 51, no. 2, pp. 523–536, Jan. 2005.

[21] A. M. Yaglom, "Some classes of random fields in n-dimensional space, related to stationary random processes," *Theory of Probability & Its Applications*, vol. 2, no. 3, pp. 273–320, Jul. 1957.

[22] Z. Wan, J. Zhu, Z. Zhang, L. Dai, and C.-B. Chae, "Mutual information for electromagnetic information theory based on random fields," *IEEE Trans. Commun.*, early access, Feb. 2023, 10.1109/TCOMM.2023.3247725.

[23] P. D. Lax, *Functional analysis*. John Wiley & Sons, 2002, vol. 55.

[24] I. Gohberg and M. G. Kreĭn, *Introduction to the theory of linear nonselfadjoint operators*. American Mathematical Soc., 1978, vol. 18.

[25] B. Simon, *Trace ideals and their applications*. American Mathematical Soc., 2005, no. 120.

[26] P. J. Davis and P. Rabinowitz, *Methods of numerical integration*. Courier Corporation, 2007.

[27] F. Bornemann, "On the numerical evaluation of Fredholm determinants," *Mathematics of Computation*, vol. 79, no. 270, pp. 871–915, Sep. 2009.

[28] C. D. Meyer, *Matrix analysis and applied linear algebra*. Siam, 2000, vol. 71.